Operando Temperature Measurements of Photovoltaic Laser Power Converter Devices Under Continuous High-Intensity Illumination

John F. Geisz, Daniel J. Friedman, Myles A. Steiner, Ryan M. France, and Tao Song

***Abstract*—Photovoltaic devices that operate under extremely high irradiances, such as laser power converters (LPCs), may also operate at elevated temperatures, even under active cooling, as the result of large temperature gradients. We demonstrate the operation of GaAs LPC devices under orders of magnitude of irradiances up to 150 W/cm^2 in a monochromatic laser simulator with an active cooling stage. The steady-state open-circuit voltage (V_{OC}) as a function of irradiance is known to droop at high irradiance as the result of junction heating, but the junction temperature can be difficult to measure by conventional methods. Fast, transient V_{OC} measurements under these extreme operating conditions are used here to determine the junction temperature. Empirical V_{OC} temperature coefficients of the devices at each irradiance of interest are determined and used as an integral part of this technique. We show that the thermal design of different LPC devices strongly affects the operating temperature of the junctions. Knowledge of the operating temperature can be a strong tool for understanding the nature of loss mechanisms and improving the design for the operation of photovoltaic LPCs at high irradiances. This technique can be used for laboratory devices during initial design as well as to characterize mass-produced and packaged devices for quality control.**

***Index Terms*—Laser power converter (LPC), optical heating, photovoltaic (PV) device, temperature measurement.**

I. Introduction

LASER power converters (LPCs) are photovoltaic (PV) devices that convert directed monochromatic light into electricity. Optical wireless power transmission over fiber optics or through free space that utilizes LPCs has many important applications to transfer energy without electrical conductors [1]. Power conversion efficiencies of GaAs LPC devices around 69% have been demonstrated [2] and efficiencies could theoretically approach 85% [3]. As optical power densities are increased, both the usefulness of practical LPC applications and the device efficiencies could potentially increase, but loss mechanisms, such as nonradiative Auger recombination and resistance (I^2R), become increasingly dominant. These loss mechanisms collectively generate heat, which further deteriorates the performance of PV devices if not effectively dissipated. Under high-intensity illumination, which is typically absorbed within the first several micrometers of LPC device depth, large thermal gradients can exist even when active cooling is utilized. The nonideal thermal properties of typical semiconductor materials (e.g., GaAs substrates) only exacerbate this problem. The proper design of LPC devices requires a thorough understanding of the optical properties of the semiconductor, which depend on the operating temperature of the p-n junction [4]. Multijunction LPC device performance can be particularly sensitive to temperature variations [5]. Understanding the heat transfer processes of packaged or cooled high-power devices under extreme operating conditions can be difficult and, sometimes, counterintuitive without careful modeling. Due to the large thermal gradients within micrometers, it is impossible to measure and, thus control, the PV junction temperature under operating conditions using conventional methods, such as thermocouples or RTD sensors.

Some previous LPC measurements have utilized a white-light flash simulator, for which the short duration of the flash (on the order of milliseconds) minimizes the heating effects during controlled characterization [2], but these measurement conditions are significantly different from the final application conditions. It is, therefore, essential to devise a method to accurately measure the temperature of PV LPC device junction within its intended operating conditions for device characterization, modeling, and design.

The open-circuit voltage (V_{OC}) of solar cells [6], [7] and thermophotovoltaic [8], [9] PV devices has long been recognized as an excellent probe of temperature since it is a strong function of temperature and irradiance [10], [11], [12] and can, thus, be used to extract the temperature of the PV junction. In this article, we present and demonstrate a practical method of determining the junction temperature under LPC operating conditions using V_{OC} as a probe.

II. Fast V_{OC} Method

When a PV device at thermal equilibrium (T_0) in the dark is suddenly illuminated, the absorption of photons leads to the generation of electron–hole pairs and the concurrent production of heat. This heat gradually accumulates in the device while it

Manuscript received 2 June 2023; revised 11 July 2023; accepted 4 August 2023. This work was supported by the Laboratory Directed Research and Development Program of the National Renewable Energy Laboratory, operated by Alliance for Sustainable Energy, LLC, for the U.S. Department of Energy under Grant DE-AC36-08GO28308. *(Corresponding author: John F. Geisz.)*

The authors are with the National Renewable Energy Laboratory, Golden, CO 80401 USA (e-mail: john.geisz@nrel.gov; daniel.friedman@nrel.gov; myles.steiner@nrel.gov; ryan.france@nrel.gov; tao.song@nrel.gov).

Color versions of one or more figures in this article are available at https://doi.org/10.1109/JPHOTOV.2023.3304360.

Digital Object Identifier 10.1109/JPHOTOV.2023.3304360

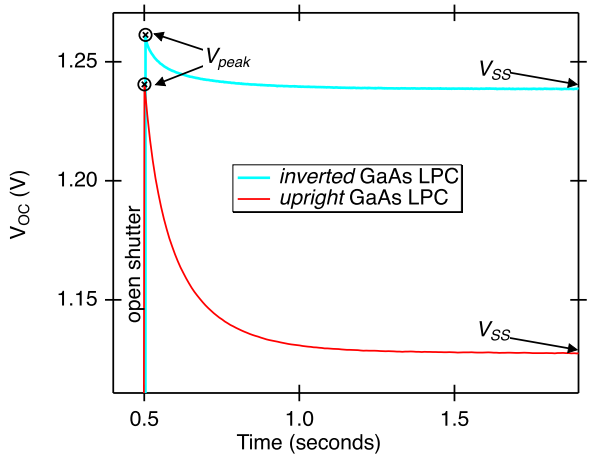

Fig. 1. Fast transient V_{OC} measurements of *inverted* (blue) and *upright* (red) GaAs 1J LPC devices under approximately 150-W/cm^2 808-nm laser illumination. The devices were mounted on a 20 °C temperature-controlled stage. Data resolution is 2–9 ms and the shutter opened at 0.5 s within 6 ms.

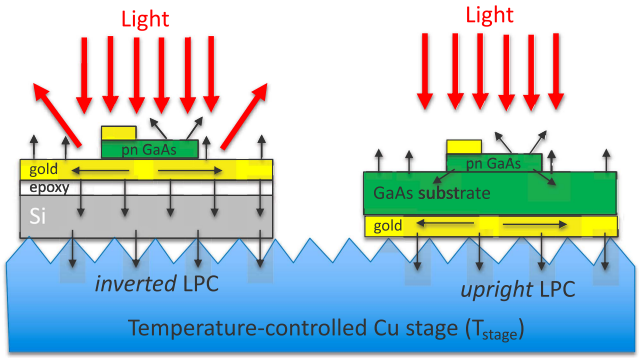

Fig. 2. Schematics of *inverted* (left) and *upright* (right) LPC device structures. The red arrows indicate optical radiation and the black arrows show various heat flow pathways.

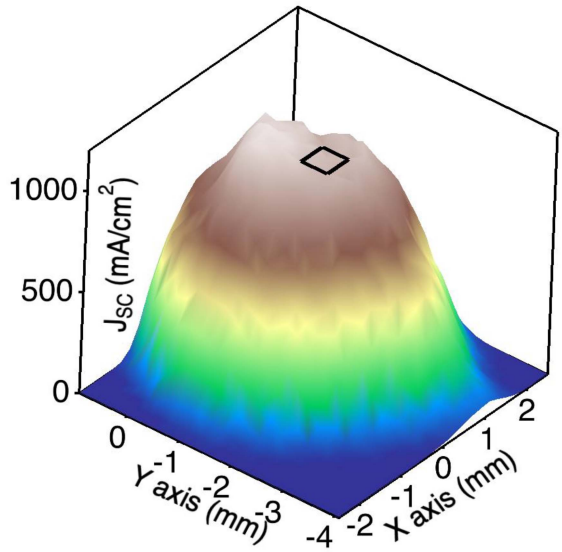

Fig. 3. Current density map of the 808-nm laser illumination spot as it was rastered over a 500 μm × 500 μm 1J GaAs LPC device. The square in the center shows the size of the device mesa in relation to the laser beam.

also dissipates to the surroundings, approaching a steady-state condition. The rate of heat flow is significantly slower than the rates of photon and electron flow, so we assume that V_{OC} of the device is a direct function of the instantaneous temperature and total irradiance (E_{tot}), with the electrons at quasi-steady state. If V_{OC} is measured quickly enough, the highest voltage V_{peak} measured immediately after illumination can be assumed to be V_{OC} (T_0, E_{tot}). Over the course of the next few milliseconds, seconds, minutes, or hours, the device heats up and V_{OC} ($T(t)$, E_{tot}) drops as a function of time as shown in Fig. 1 toward a steady-state value V_{SS} where the rate of heat extraction balances the rate of optical heating [9]. By adjusting an active cooling stage until V_{SS} is the same as V_{peak} measured at a previously controlled reference temperature (e.g., T_0 = 25 °C) [9], an *IV* curve can be acquired at the reference temperature even though the large thermal gradient still exists and the previous steady-state temperature is still unknown. Alternatively, if we know the behavior of V_{OC} as a function of temperature at a particular irradiance, we can directly determine the actual temperature at the thermal steady-state [13]. Over the typical operating temperature ranges of PV devices, this dependence is usually found to be linear and is characterized by a V_{OC} temperature coefficient.

III. Experimental

In this study, we characterize two 500 μm × 500 μm single-junction (1J) GaAs LPC devices with different structures, as shown in Fig. 2. Both GaAs PV devices were grown by organo-metallic vapor phase epitaxy with lattice-matched GaInP window and back-surface-field layers for electrical passivation. Thick window layers (nominally 1 μm) were used in order to minimize the sheet resistance in LPC devices, but no antireflective (AR) coating was applied. The main difference between the two devices is that one was grown *upright* and processed on the GaAs substrate (as is most typical) while the other was grown *inverted*, electroplated with gold, epoxied to a silicon wafer, and the GaAs substrate removed before final front-side processing [14], [15], making a thin-film device. Both devices were homojunction structures with about 100 nm n-doped emitter and thicker 2- or 3-μm p-doped base absorber. The *inverted* device was thinner than the *upright* device by design because the gold back-surface-reflector provided a double pass of light for nearly complete absorption. An *upright* 3-GaAs-junction device with thin GaAs/AlGaAs tunnel junctions, similar to the 1J *upright* device, was also fabricated and designed for current-matched junctions at 808 nm, but only the V_{OC} temperature coefficients of the 3J device are presented here.

The LPC devices were measured under 808-nm monochromatic light using a 35-W solid-state laser coupled to a reflective collimator via a fiber optic cable. The resulting light profile has a full width at half maximum of approximately 3 mm, which significantly overfills the small device area, providing fairly uniform illumination (within about ±5%) on the device, as shown in Fig. 3. The laser irradiance on the device was varied over

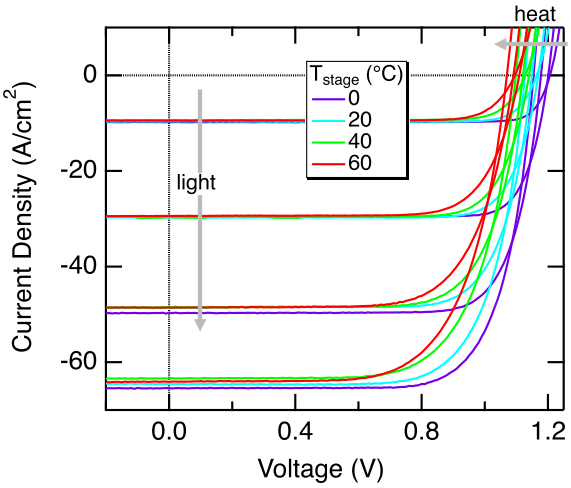

Fig. 4. Steady-state light *JV* curves of *upright* LPC device (MU836) under various irradiances of continuous 808-nm laser illumination and controlled stage temperatures (shown by color). The lowest irradiances measured are not shown here.

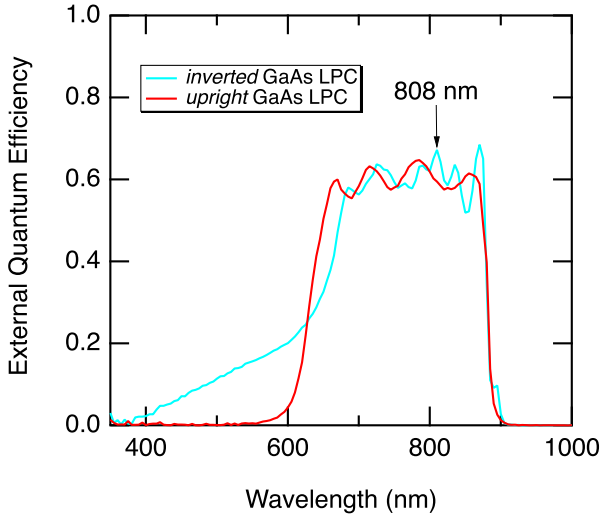

Fig. 5. EQE as a function of wavelength of *inverted* (blue) and *upright* (red) single-junction GaAs LPC devices without AR coating.

several orders of magnitude by adjusting the laser input current and adding neutral density filters at a low input current just above the laser threshold current (6 A). Light current density–voltage (*JV*) curves at various irradiance and temperatures were obtained using a source-meter unit, as shown in Fig. 4. Assuming linearity of the photocurrent with incident intensity, the total irradiance on the DUT was self-calibrated from the 1J device J_{SC} by

$$E_{tot} = \frac{J_{SC}}{\mathrm{EQE}\,(\lambda)}\frac{hc}{q\lambda} \tag{1}$$

where $\frac{hc}{q\lambda} = 1.53$ eV for the $\lambda = 808$-nm laser illumination. The external quantum efficiency (EQE) is measured using chopped light scanned through a monochromator as typical for simple PV devices. The EQE (808 nm) at 20 °C was about 60% to 67% for the devices without AR coating studied here, as shown in Fig. 5. While the EQE of these devices at 808 nm is not expected to change much with temperature, the EQE closer to the band-edge may change significantly with temperature and would, thus, need to be considered if the self-calibration of (1) is used.

Although the mesa-isolated LPC devices measured were small, the entire sample wafers with many devices were much larger (about 15 mm × 20 mm) providing better thermal contact with the stage. The full samples were vacuum-held to a nickel-plated, copper stage that was temperature-controlled between 0 and 60 °C with a thermoelectric controller. Although the devices were similar in many respects, the specifics of the lateral and vertical heat flow through thermal resistances in this setup (shown schematically in Fig. 2) resulted in different junction temperatures under high-intensity illumination, which helps to demonstrate this temperature measurement technique.

At each illumination condition and stage temperature, fast transient V_{OC} measurements [9] were also recorded as a function of time as a Uniblitz shutter was opened. This shutter is rated to completely open within 6 ms. V_{OC} was measured and recorded every 2–9 ms, as shown in Fig. 1. V_{OC} initially rises to a peak value V_{peak} that is assumed to be V_{OC} at the stage temperature T_{stage} then falls to the steady-state V_{OC} value V_{SS} over the course of several seconds. This steady-state V_{SS} from the fast V_{OC} measurement is the same as V_{OC} determined from the *JV* curves, where the temperature was stabilized at the laser irradiance for more than 20 s prior to measurement, and the voltage was typically swept from reverse to forward directions.

IV. Analysis and Discussion

The junction temperature of the cell during steady-state *JV* measurements T_{SS} was calculated at each operating condition from

$$\Delta T = (T_{SS} - T_{stage}) = \frac{\Delta V}{dV_{OC}/dT\,(J_{SC})} \tag{2}$$

where $\Delta V = (V_{SS} - V_{peak})$ from the transient measurement. V_{peak} is the maximum V_{OC} achieved immediately after opening the shutter and V_{SS} is the steady-state V_{OC} after the operating LPC device heats up to its steady-state elevated temperature under the laser irradiance used. The V_{OC} temperature coefficient, dV_{OC}/dT, is dependent on the photocurrent density that results from a particular irradiance (i.e., J_{SC} for 1J devices) [10] so it is not often straightforward to extract the value from the literature at high irradiance. Often PV V_{OC} temperature coefficients that can be found in the literature are given only at one-sun solar irradiance [16] but for some concentrating PV devices are given as a function of concentration [17], [18]. We empirically extract the dV_{OC}/dT slope from measurements of V_{peak} as a function of stage temperature [13] shown as triangles in Fig. 6 at each irradiance level (color). We also note that the data are, indeed, linear over this range as assumed. The actual junction temperature at steady state is determined from (2); thus, the shifted V_{SS} versus T_{SS} data (circles) fall on the same line as the V_{peak} versus T_{stage} data.

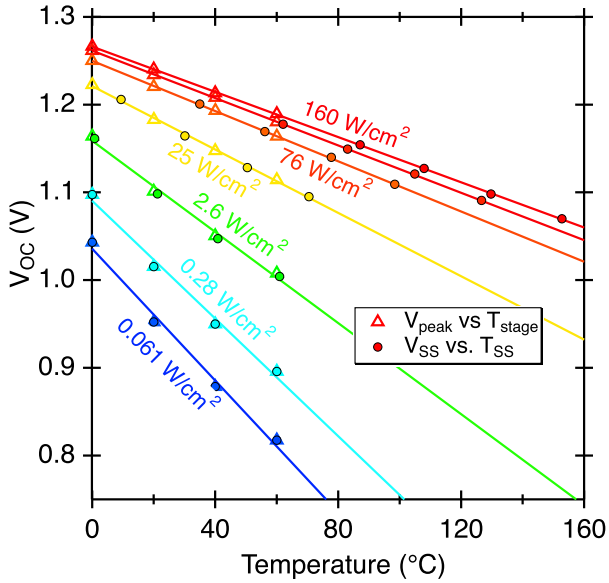

Fig. 6. dV_{OC}/dT coefficient is determined from the fit slope of V_{peak} versus T_{stage} data (triangles) at each irradiance level (labeled and indicated by color). V_{SS} is shifted to T_{SS} using (2) and shown as circle markers. Data are only shown for the *upright* LPC device (MU836) for clarity.

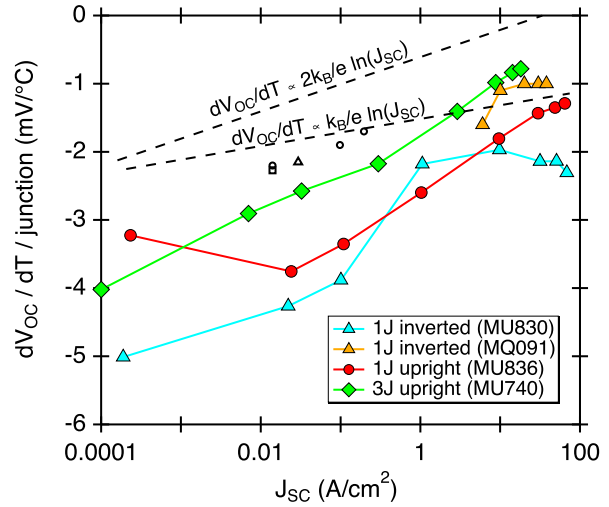

Fig. 7. V_{OC} temperature coefficient (i.e., dV_{OC}/dT) as a function of J_{SC} for several 500 μm $\times$ 500 μm GaAs LPC devices derived from slopes fit from of V_{peak} versus T_{stage} data, as illustrated in Fig. 6. The dV_{OC}/dT slope for the 3J device (green) was divided by 3 to show the dV_{OC}/dT value for each individual junction. The dashed lines show theoretical trends for $n = 1$ and 2. Open black markers indicate literature values of larger area GaAs cells (circle = [18], triangle = [11], square = [15]).

The empirically extracted dV_{OC}/dT for several GaAs devices including the two 1J devices studied here are shown as a function of J_{SC} in Fig. 7. Theoretically, the V_{OC} temperature coefficient can be understood by differentiating the diode equation

$$V_{OC} = \frac{n\,k_B T}{q} \ln\left(\frac{J_{SC}}{J_0} - 1\right) \tag{3}$$

where n is the ideality factor, k_B is Boltzmann's constant, T is the temperature, q is the elemental charge, J_0 is the reverse saturation current density, and J_{SC} is the short-circuit current density. The empirical temperature dependence of J_0 given by [11], [12], [17], [19], [20]

$$J_0 \propto T^{3/n} e^{-E_g/nk_BT} \tag{4}$$

where E_g is the bandgap. Substituting (4) into (3), differentiating and neglecting the (-1) term as well as the resulting J_{SC} temperature coefficient term (which is typically relatively small), the V_{OC} temperature coefficient can be estimated by

$$\frac{dV_{OC}}{dT} \approx \frac{1}{T}\left[V_{OC} - \frac{3nk_BT}{q} - \frac{nE_g}{q}\right] + \frac{n}{q}\frac{dE_g}{dT}. \tag{5}$$

Substituting V_{OC} from (3), we can understand the logarithmic dependence of dV_{OC}/dT with J_{SC}

$$\frac{dV_{OC}}{dT} \approx \frac{nk_B}{e}\ln(J_{SC}) - \frac{nk_B}{e}\ln(J_0) - \frac{3nk_B}{e} - \frac{nE_g}{eT} + \frac{n}{e}\frac{dE_g}{dT}. \tag{6}$$

Here, the first term gives the J_{SC} dependence of the V_{OC} temperature coefficient as shown as dashed lines in Fig. 7 for ideality factors of $n = 1$ and 2. The second term results in differences between devices based on diode quality through J_0. This term may be influenced by the junction structure and by perimeter recombination in small cells. The remaining terms depending on the bandgap are well described by the Varshi equation and are the same for all GaAs PV devices. Finally, it should be recognized that the ideality factor may itself be a function of J_{SC}, as GaAs devices often require a two-diode model. Thus, we see from Fig. 7 that the V_{OC} temperature coefficient varies between similar device structures and is a strong function of current density, so it is extremely helpful to actually measure each device design at the intended operating conditions for the lowest uncertainty in junction temperature determination.

A summary of all the V_{OC} measurements for temperature extraction of the two 1J GaAs LPC devices is shown in Fig. 8 as a function of the laser irradiance. The peak V_{OC} from transient measurements (see Fig. 1) is shown in the top panel and the steady-state V_{OC}, which is the same as the *JV* extracted V_{OC}, is shown in the second panel. The difference between these V_{OC} values is shown in the third panel, on a logarithmic scale. This V_{OC} difference is negligible and below the measurement uncertainties at low irradiances but is extremely large at high irradiances, particularly in the *upright* LPC device, where ΔV_{OC} due to heating exceeds 100 mV. The temperature rise in the last panel is calculated from (2) using the empirically determined dV_{OC}/dT values of the particular device taken from Fig. 7 as a function of the current density. The temperature rise is fairly linear with irradiance (on a log–log scale) for both devices, but the slope is very different between devices depending on how efficiently the heat is extracted. While the temperature rise at a steady state with 150-W/cm^2 laser illumination of the *inverted* GaAs LPC is only about 20 °C, the temperature of the *upright* GaAs LPC device rises by about 100 °C.

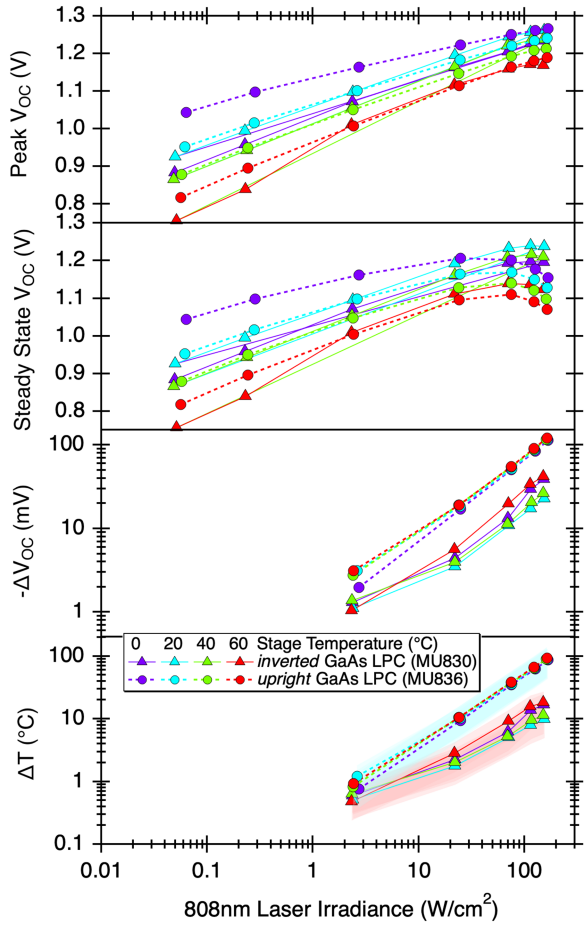

Fig. 8. Peak (top panel) and steady-state (second panel) V_{OC} as a function of irradiance (bottom axis) and stage temperature (color). The V_{OC} difference (third panel) and temperature rise (bottom panel) calculated from (2) using dV_{OC}/dT from Fig. 7. Data for *inverted* (triangles) and *upright* (circles) GaAs LPC devices are both shown. Uncertainty of ΔT is indicated by shading for *inverted* (pink) and *upright* (blue) assuming 50% uncertainty in dV_{OC}/dT.

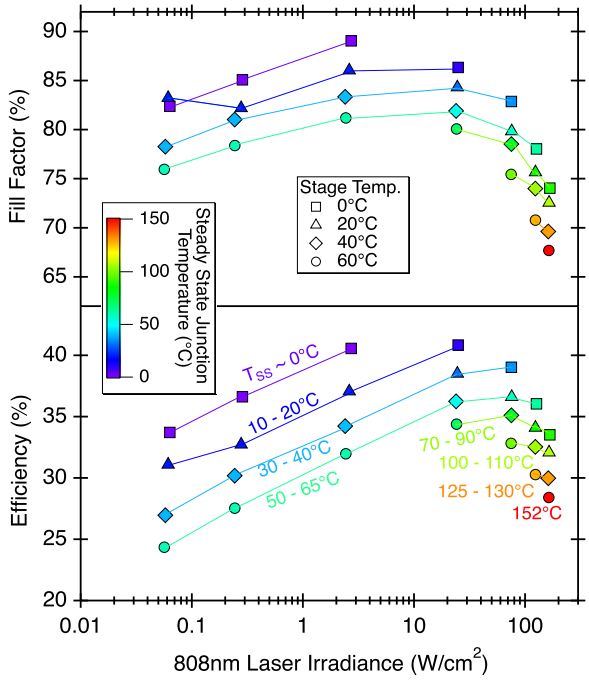

Fig. 9. Fill factor and efficiency of *JV* curves of the *upright* GaAs LPC device shown in Fig. 4 as a function irradiance (bottom axis), controlled stage temperature (marker), and calculated steady-state junction temperature (color). Lines are inserted and labeled to guide the eye between similar steady-state junction temperatures.

The relative uncertainty of ΔT from (2) is given by

$$\frac{U(\Delta T)}{\Delta T} = \sqrt{\left(\frac{U(\Delta V_{OC})}{\Delta V_{OC}}\right)^2 + \left(\frac{U(dV_{OC}/dT)}{dV_{OC}/dT}\right)^2}. \quad (7)$$

While the relative uncertainty of ΔV_{OC} is limited by the speed and accuracy of the transient V_{OC} measurement to determine V_{peak}, this uncertainty term is typically quite small compared to the second term whenever ΔV_{OC} is above the noise. The uncertainty in the junction temperature derived by this method is, therefore, dominated by the uncertainty of dV_{OC}/dT. Any degradation or instability in device performance as the temperature is changed to make this measurement makes the accurate determination of dV_{OC}/dT difficult. Measurement of devices at high temperatures and irradiances to cover the range of interest could cause them to degrade slightly in voltage performance. Thus, the importance of careful empirical measurement of dV_{OC}/dT is evident for highly accurate temperature determination. Even assuming high relative uncertainties in dV_{OC}/dT (perhaps as high as 50% based on the spread in Fig. 7), it is clear from the order-of-magnitude difference in ΔV_{OC} in Fig. 8 that there is a significant difference in the heating of the two 1J LPC devices studied here.

While the low thermal conductivity (0.95 W/m/K from TRA-bond 2151 spec sheet) of the ~10-μm-thick epoxy layer would intuitively suggest poor heat dissipation in the *inverted* LPC device shown schematically in Fig. 2(left), it may be that the very effective lateral heat transport through the ~1-μm-thick gold (318 W/m/K) away from the laser-illuminated area allows it to remain cooler than the *upright* LPC device, which is limited by the 300-μm-thick GaAs substrate (56 W/m/K) with thermal conductivities much less than gold. In addition, the area around the small cell of the inverted LPC is a highly reflective back-contact gold, which prevents much of the beam outside the device area from being absorbed by the substrate. The machined temperature stage is, upon close inspection, very jagged, preventing close contact with the flat sample back, so thermal pastes may improve the thermal contact of both devices. Detailed three-dimensional thermal modeling of these devices could better elucidate these results but it is beyond the scope of this article.

In a well-designed LPC package, excellent thermal extraction is of primary importance. The temperature of the package may not be actively controlled, but if the LPC package temperature can be measured at thermal equilibrium with the laser OFF, then this technique can be used with similar fast V_{OC} measurements after turning the laser ON. This technique for the *operando* temperature measurement could confirm and quantify the efficacy of the thermal packaging of the LPC device.

Finally, the fill factor (FF) and efficiency of the measured *JV* curves (*upright* device only) are summarized in Fig. 9.

The efficiency of the 1J LPC device was determined by [2]

$$\eta = \frac{P_{\text{out}}}{E_{\text{tot}}} = \frac{V_{\text{mpp}}\ J_{\text{mpp}}}{J_{\text{SC}}} \frac{q\lambda}{hc} \text{EQE}\,(\lambda) \tag{8}$$

where V_{mpp} and J_{mpp} are the voltage and current density at the maximum power point of the *JV* curve, respectively. Note that while this technique can also be used for vertical multijunction LPCs [21], the second equality of (8) is invalid for stacked multijunction LPC devices, due to different EQEs in each junction. A multijunction LPC requires E_{tot} to be determined with a separate 1J calibration device for the efficiency calculation.

The fill factor and efficiency data in Fig. 9 are parameterized as a function of both the controlled stage temperature (shown by symbol) and by the junction temperature determined from this method (shown by color and connected with guiding lines). The significant drop in (FF) and efficiency that occurs at high irradiances at a constant stage temperature can now be seen to be largely the result of voltage loss due to sample heating of this device. The remaining drop in FF and efficiency at high irradiance can be attributed to resistive losses. Separating these two loss mechanisms is essential for the optimization of LPC device designs for high irradiance operation. For example, it is clear from Fig. 9 that the efficiency of this *upright* LPC at high irradiance could be greatly improved just by improving the heat extraction.

V. Conclusion

This article describes an invaluable technique to determine the junction temperature of PV LPC devices under continuous monochromatic illumination even at very high irradiances in their typical operating conditions. The V_{OC} temperature coefficient is determined empirically in this technique as a function of J_{SC} so no assumptions must be made about the device properties. We have quantified significant differences in the thermal design of two similar GaAs LPC devices using this technique. Knowledge of the true steady-state junction temperature elucidates the mechanisms of power loss at high irradiances and could accelerate the development of thermal packaging for improved optical power transfer efficiencies.

Acknowledgment

The authors thank Michelle Young and Sarah Collins for device fabrication; Kevin Schulte, Nikos Kopidakis, and Stephen Gorin for discussions, and for support of this work and its dissemination for further business development. The views expressed in the article do not necessarily represent the views of the DOE or the U.S. Government. The U.S. Government retains and the publisher, by accepting the article for publication, acknowledges that the U.S. Government retains a nonexclusive, paid-up, irrevocable, worldwide license to publish or reproduce the published form of this work, or allow others to do so, for U.S. Government purposes.

References

[1] C. Algora et al., "Beaming power: Photovoltaic laser power converters for power-by-light," *Joule*, vol. 6, pp. 1–29, 2021.
[2] H. Helmers et al., "68.9% efficient GaAs-based photonic power conversion enabled by photon recycling and optical resonance," *Phys. Status Solidi RRL*, vol. 15, 2021, Art. no. 2100113.
[3] S. D. Jarvis, "Towards high efficiency photovoltaics for applications in laser power beaming," Ph.D. dissertation, Univ. Surrey, Guildford, U.K., Jul. 2017. [Online]. Available: https://www.proquest.com/openview/633120259c8551f337b5da2ca6cc1325/1?pq-origsite=gscholar&cbl=2026366
[4] O. Hohn, A. W. Walker, A. W. Bett, and H. Helmers, "Optimal laser wavelength for efficient laser power converter operation over temperature," *Appl. Phys. Lett.*, vol. 108, 2016, Art. no. 241104.
[5] S. K. Reichmuth et al., "On the temperature dependence of dual-junction laser power converters," *Prog. Photovolt.: Res. Appl.*, vol. 25, pp. 67–75, 2017.
[6] D. H. Levi et al., "Self-reference procedure to reduce uncertainty in module calibration," in *Proc. IEEE 44th Photovolt. Specialists Conf.*, 2017, pp. 467–471, doi: 10.1109/PVSC.2017.8366752.
[7] *Photovoltaic Devices - Part 5: Determination of the Equivalent Cell Temperature (ECT) of Photovoltaic (PV) Devices by the Open-Circuit Voltage Method*, Standard IEC 60904-5, IEC, Geneva, Switzerland, 2011.
[8] K. Emery, "Characterizing thermophotovoltaic cells," *Semicond. Sci. Technol.*, vol. 18, pp. S228–S231, 2003.
[9] T. Moriarty and K. Emery, "Thermophotovoltaic cell temperature measurement issues," *AIP Conf. Proc.*, vol. 460, pp. 301–311, 1999.
[10] A. Braun, E. A. Katz, and J. M. Gordon, "Basic aspects of the temperature coefficients of concentrator solar cell performance parameters," *Prog. Photovolt.: Res. Appl.*, vol. 21, pp. 1087–1094, 2013.
[11] J. C. C. Fan, "Theoretical temperature dependence of solar cell parameters," *Sol. Cells*, vol. 17, pp. 309–315, 1986.
[12] G. S. Kinsey et al., "Concentrator multijunction solar cell characteristics under variable intensity and temperature," *Prog. Photovolt.*, vol. 16, pp. 503–508, 2008.
[13] R. M. France and M. A. Steiner, "High-irradiance degradation studies of metamorphic 1eV GaInAs solar cells," *MRS Online Proc. Library*, vol. 1432, pp. 105–110, 2012.
[14] J. F. Geisz et al., "High-efficiency GaInP/GaAs/InGaAs triple-junction solar cells grown inverted with a metamorphic bottom junction," *Appl. Phys. Lett.*, vol. 91, 2007, Art. no. 023502.
[15] M. A. Steiner et al., "Optical enhancement of the open-circuit voltage in high quality GaAs solar cells," *J. Appl. Phys.*, vol. 113, 2013, Art. no. 123109.
[16] M. A. Steiner et al., "Temperature-dependent measurements of an inverted metamorphic multijunction (IMM) solar cell," in *Proc. 37th IEEE Photovolt. Specialists Conf.*, 2011, pp. 002527–002532, doi: 10.1109/PVSC.2011.6186461.
[17] H. Helmers, M. Schachtner, and A. W. Bett, "Influence of temperature and irradiance on triple-junction solar subcells," *Sol. Energy Mater. Sol. Cells*, vol. 116, pp. 144–152, 2013.
[18] K. Nishioka et al., "Evaluation of temperature characteristics of high-efficiency InGaP/InGaAs/Ge triple-junction solar cells under concentration," *Sol. Energy Mater. Sol. Cells*, vol. 85, pp. 429–436, 2005.
[19] E. E. Perl et al., "Measurements and modeling of III-V solar cells at high temperatures up to 400°C," *IEEE J. Photovolt.*, vol. 6, no. 5, pp. 1345–1352, Sep. 2016.
[20] D. J. Friedman, "Modelling of tandem cell temperature coefficients," in *Proc. 25th IEEE Photovolt. Specialists Conf.*, 1996, pp. 89–92, doi: 10.1109/PVSC.1996.563954.
[21] S. Fafard et al., "Ultrahigh efficiencies in vertical epitaxial heterostructure architectures," *Appl. Phys. Lett.*, vol. 108, 2016, Art. no. 071101.